2014 IEEE International Conference on Robotics & Automation (ICRA)
Hong Kong Convention and Exhibition Center
May 31 - June 7, 2014. Hong Kong, China

Robot-aided Optical Manipulation of Cells with a Unified Controller*

Xiangpeng Li and Dong Sun

Abstract—**In cell manipulation with optical tweezers, it is required that the cell must be located within the optical trap. Due to the lack of a control technique that can automatically locate the cell within the optical trap while controlling the cell motion, the cell will easily escape from the optical trap and hence the manipulation task is failed. Therefore, development of a unified controller that can control both cell trapping and cell motion simultaneously has received increased attention in optical cell manipulations. In this paper, we addressed this challenging problem by developing a novel visual based control method that controls both cell positioning and cell trapping simultaneously. We first established a new geometric model aiming for confining the cell within a local region near the optical trap, and then formulated a so-called Cell-Tweezers Coalition (C-T Coalition). We secondly developed a potential field function based controller to drive the C-T Coalition to the desired position while avoiding collisions with any other obstacles in environment. Finally, we performed experiments of transferring yeast cells to demonstrate the effectiveness of the proposed approach.**

I. Introduction

Manipulation of live cells at the single cell level has inspired a lot of interests in both biology and medicine. Several experimental techniques have been developed for micromanipulation, such as micropipette aspiration [1-2], atomic force microscope [3], microfabricated cell pusher [4], microinjection [5] and magnetic tweezers [6-7]. Recently, micromanipulation technology with optical tweezers has attracted considerable attentions. Optical tweezers uses a tightly focused low-power laser beam to manipulate the microscopic particles, and exhibits advantages such as precise and non-contact manipulation manner, and producing little damage to the transferred biomedical objectives [8-10]. Optical tweezers can function as a special robot manipulator to trap and manipulate particles, in the order of piconewtons and nanometers in a noncontact manner [9, 11]. Optical trapping works only when the particles locate inside a certain area near the centroid of the focused laser beam [12].

Most of cell manipulation systems equipped with optical tweezers are operated manually so far. In [13-15], an open loop control strategy was adopted to transfer cells along pre-designed collision-free paths. Similar methods was reported in [16], where an A* motion planner was proposed to transfer a single cell. In [17], a simple feedback control scheme was proposed to transfer micro particles. A closed loop control strategy, reported in [18], automatically manipulated single as well as multiple cells in obstacle-free environment. In [19], a region based flocking control strategy was proposed to manipulate multiple cells in formations. All these works assumed that the cell was located near the trapping center of the laser beam in the control design. A recent effort aiming to control both cell trapping and cell manipulation in obstacle-free environment was reported in [20].

In cell manipulation with optical tweezers, the trapped cell may easily escape from the optical trap, which causes the manipulation task to fail. In the current paper, we developed a novel solution to overcome this problem. Motivated by our formal works on connectivity control in networked robots [21-22], we proposed a unified controller that controls cell trapping, cell positioning and collision avoidance simultaneously. To achieve this goal, we firstly proposed a new geometrical model that confines the cell within a local region around the center of the optical trap, and based on this model we established the geometrical constraint for the trapped cell. Secondly, we proposed a new concept, termed the Cell-Tweezers (C-T) Coalition, to define the connection between the cell and the optical trap. Then, we designed a potential field function based feedback controller to drive such a C-T Coalition to the desired position, while keeping collision free with the other particles in environment.

Compared to the existing works, the proposed method employs a unified controller aiming for solving cell trapping, cell manipulation and obstacle avoidance simultaneously in optical manipulation of cells. The approaches proposed in [16, 18, 19] solved the cell manipulation but failed to address the cell trapping problem. Compared to the approach in [20], our controller can solve the problem of obstacle avoidance, which makes the controller easily applied to practical applications.

II. Manipulation System

Figure 1 illustrates a robot-assisted optical tweezers system for cell manipulation. The system includes a diode laser (808 nm, 2 W), a CCD camera, a microscope objective, a X-Y motorized stage (PIM-111.1DG) and a host computer. The cells are contained in a slide placed on the motorized stage. The laser beam produced by the laser passes through a beam expander, reflected by the dichroic mirror, and finally focused on the sample in the slide. The optical tweezers is fixed, and the relative movement between the cell and the sample holder can be accomplished by moving the stage. Position of the cell can be obtained through image processing

*This research was supported in part by grants from Research Grants Council of the Hong Kong Special Administrative Region, China [Reference No. CityU 120709 and CityU9/CRF/13G]

X. Li is with the Department of Mechanical and Biomedical Engineering, City University of Hong Kong, Kowloon, Hong Kong (e-mail: xiangpli@cityu.edu.hk)

D. Sun is with the Department of Mechanical and Biomedical Engineering, City University of Hong Kong, Kowloon, Hong Kong (phone: +852 3442-8405; fax: +852 3442-0176; e-mail: medsun@cityu.edu.hk).

with the visual feedback from a CCD camera. All components of the system are supported upon an action isolated platform.

The control strategy for cell manipulation is shown in Fig. 2. In the initial phase, image processing technology is used to detect the environment information including the positions of cells and any other bio-tissues. Then, the target cell is labeled by the operator, and trapped by the optical tweezers automatically. The destination of the trapped cell is assigned through the software interface. Finally, the cell is transferred to the destination with the proposed control algorithm.

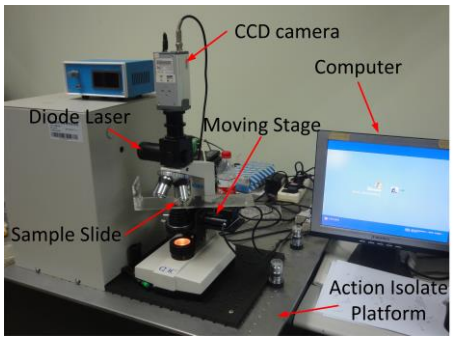

Figure 1. Robot-aided cell manipulation system with optical tweezers.

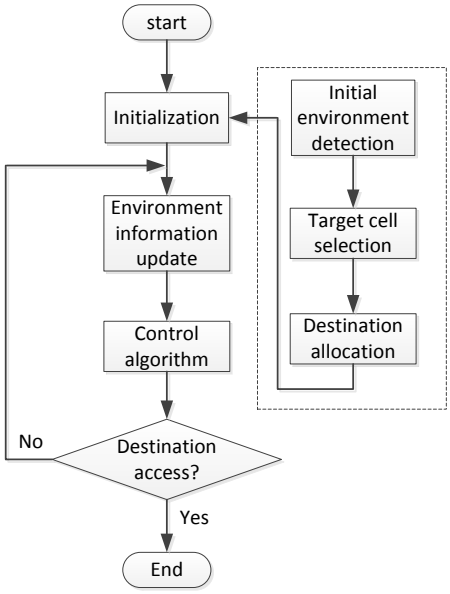

Figure 2. Control scheme.

Denote the cell as a sphere centered at $q(t)\in\Re^2$ with radius of R_C, and the destination the cell moves towards as g. Similarly, denote the laser trap as a sphere too, centered at $l(t)\in\Re^2$ with radius of r. The main forces that govern the motion of the trapped cell consist of the trapping force F_{trap} caused by the optical trap and the viscous drag force F_{drag} caused by the liquid, as reported in [18, 23]. The dynamics of the trapped cell is then given by

$$m\ddot{q} = F_{trap} - F_{drag} = a(l-q) - b\dot{q} \tag{1}$$

where $F_{drag} = b\dot{q}$ representing the viscous drag force, and b denotes the viscous coefficient; $F_{trap} = a(l-q)$ representing the trapping force as shown in Fig. 3, and a denotes the trapping stiffness. Note that $l-q$ denotes the offset between the centroid of the target cell and the focus of the laser beam. As seen in Fig. 3, the trapping force increases approximately linearly as the offset increases when $\|l-q\| \le r_0$, and the trapping force decreases approximately linearly as the offset increases when $\|l-q\| > r_0$. The trapping force becomes zero when the cell is completely outside the trap. Therefore, it is ideal to confine the trapped cell within a neighbored of the laser beam to prevent the cell escaping from the optical trap during manipulation [18-19]. This neighborhood can be represented as the trapping area formulated as follows

$$\mathrm{C} = \left\{ q \middle| r_0^{\,2} - \|l-q\|^2 > 0 \right\} \tag{2}$$

where r_0 denotes the critical offset [18-19].

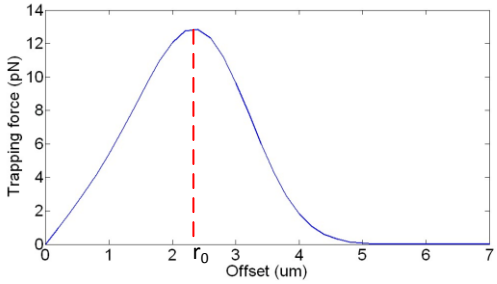

Figure 3. Trapping force versus offset based on yeast cell tests [18].

In the liquid environment with a low Reynolds number, the effect of the inertia force $m\ddot{q}$ is very small and hence can be ignored [18, 22]. In this study, the maximum Reynolds number is $3\times10^{-4} << 1$, and the effect of the inertia force $m\ddot{q}$ can be ignored. The dynamics of the motion of the cell is then simplified as

$$\dot{q} = \frac{a}{b}(l-q) \tag{3}$$

III. Modeling

A. Cell-tweezers (C-T) coalition

Fig. 4 illustrates the cell in optical trap. The target cell is denoted with a sphere with solid line, and the optical trap is denoted as a sphere with dotted line. The optical tweezers can trap the cell only when the centroid of the cell locates inside the trapping area C, which is denoted as the solid circle in Fig. 4 (a). In other words, the center of the laser beam should be controlled to stay "connected" with the trapped cell by maintaining the cell always located inside the trapping area C during the manipulation. Such a Cell-Tweezers (C-T) connection pair is defined as a Cell-Tweezers Coalition (C-T coalition) in this paper, sharing a similar coalition idea to the multirobot connectivity control in our previous works [21].

Introduce a constraint function for maintaining the C-T coalition as follows

$$G_{C-T} = \frac{1}{2}\left(r_0^{\,2} - \|l - q\|^2\right) \tag{4}$$

Note that $G_{C-T} > 0$ means the C-T coalition is maintained, indicating that the cell is maintained within the optical trap.

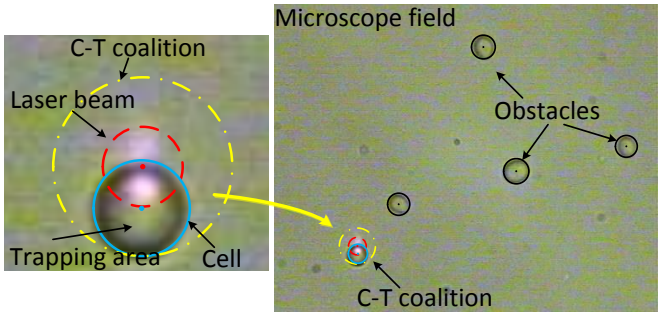

Figure 4. Illustration of C-T coalition modeling.

Utilizing the C-T coalition constraint function, the C-T coalition can be considered as a virtual sphere defined as follows.

Definition 1 (C-T coalition) The C-T coalition is defined as a virtual sphere centered at l with radius of R_{C-T}, meeting the C-T coalition constraint $G_{C-T} > 0$.

B. Obstacle avoidance

We now consider collision avoidance between the C-T coalition and the other particles. Denote all other particles are as sphere obstacles, centered at q_ς with radius of R_ς for $\varsigma \in \{1,\cdots,m\}$. Introduce a constraint function for obstacle avoidance, expressed as

$$G_O = \prod_{\varsigma=1}^{n}\left(\frac{1}{2}\left(\|l - q_\varsigma\|^2 - \left(R_{C-T} + R_\varsigma\right)^2\right)\right) = \prod_{\varsigma=1}^{n}\alpha_\varsigma \tag{5}$$

If $G_O > 0$, there is no collision between the C-T coalition and the other particles during manipulation.

With integration of the C-T coalition constraint and the obstacle avoidance requirments, a new workspace termed *free coalition manipulation space* is defined as follows:

Definition 2 (Free coalition manipulation space)

$$F = \left\{l \middle| G = G_{C-T}G_O > 0\right\} \tag{6}$$

In the mentioned space F, the target cell locates within the optical trap to maintain the C-T coalition, and meanwhile, the coalition remains collision-free.

Denote $u = \dot{l} \in \Re^2$ as the velocity of the optical tweezers, which is also the control input. We then formulate the coalition manipulation problem as follows:

Consider the cell manipulation system with dynamics (3). Under the initial configuration $G(0) > 0$, determine the control input u to drive the target cell to a desired position g while maintaining $G(t) > 0,\ \forall t > 0$.

IV. Control Design

A bounded potential field $\varphi \in [0, 1]$ is designed to drive the C-T coalition to the desired position, expressed by

$$\varphi = \frac{\gamma}{\left(\gamma^\delta + G\right)^{\frac{1}{\delta}}} \tag{7}$$

where δ is a positive parameter, $\gamma = \frac{1}{2}e_{C-T}{}^T e_{C-T}$ is a criteria function, and $e_{C-T} = l - g$ representing the position error of the C-T coalition. The control input is designed as a negative gradient of the potential function φ, expressed by

$$u = -k\frac{\partial\varphi}{\partial l} \tag{8}$$

where k is a positive control gain.

Theorem 1 Consider a cell manipulation system equipped with optical tweezers and subjected to dynamics (3). Under the initial configuration of $G(0) > 0$, the control law (8) gives rise to: i) $G(t) > 0,\ \forall t > 0$; ii) The trapped cell is confined within the optical trap; iii) The C-T coalition is obstacle-free.

Proof: Denote $\nabla_l G$ as the gradient of G, thus, the vector $\nabla_l G$ is norm to the boundary of the free coalition manipulation space ($G = 0$) and towards the internal of F ($G > 0$). Taking the inner product of vectors u and $\nabla_l G$, we have

$$\begin{aligned} & u\nabla_l G \\ &= k\left(\gamma^\delta + G\right)^{-\frac{1}{\delta}-1}\left(\frac{\nabla_l\gamma^T\nabla_l\gamma\nabla_l G^T\nabla_l G}{2\delta} - G\nabla_l\gamma\nabla_l G\right) \\ &\geq k\|\nabla_l\gamma\|\|\nabla_l G\|\left(\gamma^\delta + G\right)^{-\frac{1}{\delta}-1}\left(\frac{\|\nabla_l\gamma\|\|\nabla_l G\|}{2\delta} - G\right) \end{aligned} \tag{9}$$

The following shows that the constraint condition (6) will always be maintained. If the constraint condition (6) is broken and the center of laser beam locates very close to the boundary of the free coalition manipulation space, either of the following two cases holds.

Case 1: The target cell escapes from optical trap, and the center of the laser beam almost locates outside the boundary of free coalition manipulation space formed by $G_{C-T} > 0$. then we have $0 < G_{C-T} < \frac{\xi}{2}$, where ξ denotes a sufficient small positive value.

Case 2: The C-T coalition collides with the ςth obstacle, and we have $0 < \alpha_\varsigma < \frac{\xi}{2}$.

In case 1, we have $\lim_{\xi \to 0} G_{C-T} = 0$, and furthermore,

$$\left\| \nabla_l G \right\| = \lim_{\xi \to 0} \left\| G_O (q - l) + \sum_{\varsigma=1}^{m} G_{C-T} \bar{\alpha}_\varsigma (l - q_\varsigma) \right\| = G_O r_0 \quad (10)$$

where $\bar{\alpha}_\varsigma = \prod_{\tau \neq \varsigma} \alpha_\tau$, and $\tau \in \{1, \cdots, m\}$. Substituting (10) into (9) yields

$$u \nabla_l G > \frac{k \left(G_O r_0 \| e_{C-T} \| \right)^2}{2\delta \left(\gamma^\delta \right)^{\frac{1}{\delta}+1}} > 0 \quad (11)$$

Inequality (11) implies that when the target cell locates closely to the boundary of free coalition manipulation space formed by $G_{C-T} = 0$, the angle between the velocity and the vector $\nabla_l G$ is acute angle. This result indicates that the velocity of the optical tweezers agrees with the vector $\nabla_l G$ and the cell converges to the internal of F. It therefore follows that $0 < G_{C-T} < \frac{\xi}{2}$ never happens, and thus, $G_{C-T} < \frac{\xi}{2}$.

In case 2, the similar result to case 1 can be obtained, and the proof is omitted.

It is finally concluded that $G(t) > 0, \forall t \geq 0$. The optical tweezers can adaptively adjust its motion to maintain the target cell within the optical trap while avoiding collisions with the other particles.

■

Lemma 1 A positive lower bound δ exists on parameter δ (see (7)) such that the desired position g is the only critical point for the C-T coalition in the free coalition manipulation space.

Proof: Please refer to [21] for details. Following the conclusion in [21], the lower bound on δ can be expressed as

$$\hat{\delta} = \frac{e_{C-T}}{2} \left(\frac{r_0}{G_{C-T}} + \sum_{\varsigma=1}^{m} \frac{\| l - q_\varsigma \|}{\alpha_\varsigma} \right) \quad (12)$$

where $\hat{\delta}$ denotes the lower bound on δ. In practical applications, we can choose the lower bound for δ.

■

Theorem 2 Consider a cell manipulation system equipped with optical tweezers, with initial configuration of $G(0) > 0$. The controller (8) gives raise to: i) system (3) is global asymptotic stable; ii) $e_{C-T} \to 0$ asymptotically as $t \to \infty$; iii) $e \to 0$ asymptotically as $t \to \infty$, where $e = q - g$ denotes the position error of the target cell.

Proof: See Appendix A.

■

V. SIMULATION

A simulation was performed on manipulating the yeast cell to demonstrate the proposed control approach. The parameters of the yeast cell and optical tweezers were chosen as [23]: the critical offset was $r_0 = 2.0 \mu m$, and the trap stiffness on yeast cell was calibrated as $a = 0.6 pN/\mu m$. Drag coefficient of blood was calibrated as $b = 0.358 pN/(\mu ms)$ at 25 degrees centigrade.

As shown in Fig. 5 (a), the yeast cell was denoted by the big circle, and the laser beam was denoted as the small circle. The initial position of the target cell was $q(0)$=[$0\mu m$, $0\mu m$]^T. The destination was denoted by crosses with configurations of g=[$25\mu m$, $30\mu m$]^T. Six obstacles were positioned in the workspace, denoted by disks with configuration of q_1=[$5\mu m$, $15\mu m$]^T, q_2=[$20\mu m$, $30\mu m$]^T, q_3=[$15\mu m$, $30\mu m$]^T, q_4=[$25\mu m$, $20\mu m$]^T, q_5=[$30\mu m$, $0\mu m$]^T, and q_6=[$0\mu m$, $25\mu m$]^T. The sampling period was chosen as 1ms in the simulation. The feedback control gain was set as $k = 20$.

Fig. 5 illustrates the cell transformation process under the proposed controller (8), where the motion trajectory of the trapped cell is denoted by the solid curve. Figs. 5 (a)-(c) illustrate the manipulation evolution at different times. Fig. 5 (d) shows that the cell manipulation task was achieved successfully.

Fig. 6 illustrates the control performance under the controller (8). Fig. 6 (a) illustrates the position error of the trapped cell in both x and y axes. All the position errors converged to zero, implying the success of the coalition manipulation task. Fig. 6 (b) illustrates the offset $\| l - q \|$ during the manipulation. The maximum value was below $2\mu m$, implying that the cell was trapped consistently during manipulation.

VI. EXPERIMENT

Since the optical tweezers was fixed in the equipment setup, the manipulation maneuver was accomplished by moving the stage in the experiment. As illustrated in Fig. 4, a transformation matrix that transforms the control input of the optical tweezers to the velocity control input of the moving stage was formulated as follows

$$u' = \begin{bmatrix} -1 & 0 \\ 0 & -1 \end{bmatrix} \begin{bmatrix} 1 & 0 \\ 0 & \cos(-\pi) \end{bmatrix} u = \begin{bmatrix} -1 & 0 \\ 0 & 1 \end{bmatrix} u \quad (13)$$

where u' denotes the velocity control input of the moving stage.

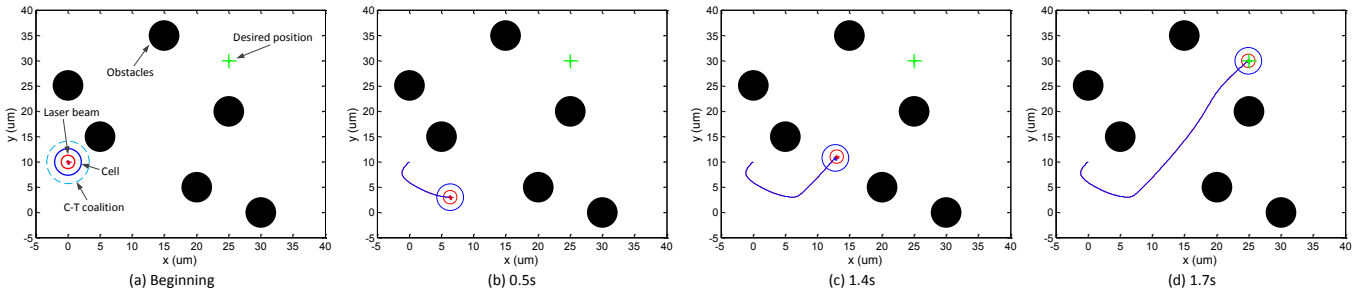

Figure 5. Coalition manipulation of cells with optical tweezers.

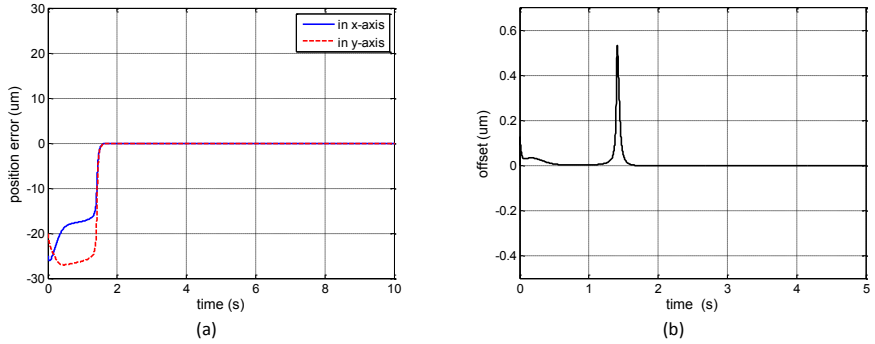

Figure 6. Control performance. a) Position error; b) Offset.

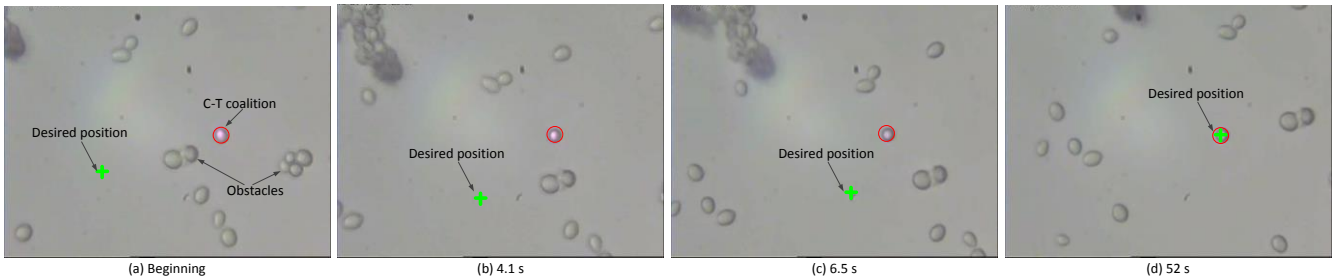

Figure 7. Coalition manipulation of yeast cells.

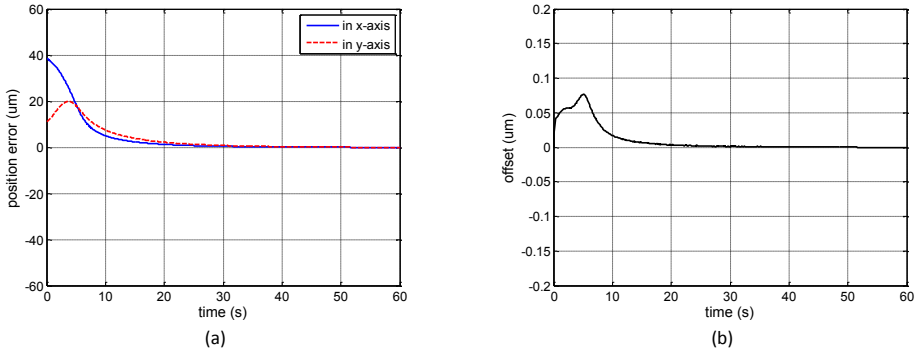

Figure 8. Control performance. a) Manipulation performance; b) Offset during manipulation.

Fig. 7 illustrates the manipulation process recorded by a video. The trapped cell was enclosed by the circle with solid line, and the target position was denoted by a cross. Other cells and particles were treated as obstacles in the workspace. Fig. 7 (a) illustrates the initial configuration, and Figs. 7 (b)-(c) show the manipulation process at different times. Fig.7 (d) shows that the cell manipulation task was achieved successfully.

The control performance of the proposed controller is shown in Fig. 8. Fig. 8 (a) illustrates that the position errors of the target cell decreased to zero, implying that the coalition manipulation task was completed successfully. Fig. 8 (b)

illustrates the variation of offset $\|l-q\|$ during the manipulation. It is seen that the offset was well confined within the critical offset r_0 during the manipulation, implying that the cell was trapped by the laser beam all the time.

VII. Conclusion

The current paper presented a novel unified controller for efficient manipulation of cells with robotically controlled optical tweezers. The proposed approach could transfer the target cell to the destination while locating cell within the optical trap consistently, and avoid collisions to the other particles during the manipulation. The proposed unified controller was based on employment of a novel geometric model, termed C-T coalition, aiming to confine the cell within the optical trap, with further consideration of obstacle avoidance. Compared to the existing control approaches for cell manipulation, the proposed unified controller could control the cell positioning, cell trapping and obstacles avoidance simultaneously. Simulation and experiment conducted on transferring the yeast cell demonstrated the effectiveness of the proposed control approach.

Appendix

Define $V=\varphi$ as the Lyapunov function candidate. Differentiating V with respect to time yields

$$\dot{V}=u\frac{\partial\varphi}{\partial l}-\frac{\gamma G_O(l-q)}{\delta\left(\gamma^{\delta}+G\right)^{\frac{1}{\delta}+1}}\dot{q} \tag{14}$$

Substituting (3) and (8) into (14) yields

$$\dot{V}=-k\left(\frac{\partial\varphi}{\partial l}\right)^2-\frac{a\gamma G_O}{\delta b\left(\gamma^{\delta}+G\right)^{\frac{1}{\delta}+1}}(l-q)^2\le 0 \tag{15}$$

Therefore, system (3) is global asymptotic stable under the controller (8). From Lemma 1, we know that $\dot{V}=0$ holds only at the equilibrium g. Therefore, the C-T coalition converges to the destination g asymptotically, and $e_{C-T}\to 0$ as $t\to\infty$.

Consider a potential energy function $V'=\frac{1}{2}\|l-q\|^2$ as a Lyapunov function candidate. Taking the time derivative of V', we have

$$\dot{V}'=-\frac{a}{b}(q-l)^2\le 0 \tag{16}$$

$V'=0$ holds at $q=l=g$. Thus, $e\to 0$ as $t\to\infty$, and q converges to g asymptotically. ■

References

[1] G. Y. H. Lee, and C. T. Lim, "Biomechanics approaches to studying human diseases". *Trends Biotechnol.*, 25, pp.111-118, 2007.

[2] R. M. Hochmuth, "Micropipette aspiration of living cells", *J. Biomechanics*, 33, pp. 15-22, 2000.

[3] M. Radmacher, "Measuring the elastic properties of biological samples with the AFM", *IEEE Engineering in Medicine and Biology Magazine*, 16, pp.47-57, 1997.

[4] M. Boukallel, M. Gauthier, M. Dauge, E. Piat, and J. Abadie, "Smart microrobots for mechanical cell characterization and cell convoying", *IEEE Trans. Biomed. Eng.*, 54, pp.1536-1540, 2007.

[5] Y. Shen, U. C. Wejinya, N. Xi, and C. A. Pomeroy, "Force measurement and mechanical characterization of living drosophila embryos for medical study", *Proc. Inst. Mech. Eng. Part H-J. Eng. Med.*, 221, pp.99-112, 2007.

[6] C. Bergeles, B. E. Kratochvil, and B. J. Nelson, "Visually servoing magnetic intraocular microdevices", *IEEE Trans. Robotics*, 28 (4), pp. 798-809, 2012.

[7] E. Diller, J. Giltinan, and M. Sitti, "Independent control of multiple magnetic microrobots in three dimensions", *The Int. J. of Robotics Research*. 32(5), pp.614-631, 2013.

[8] A. G. Banerjee, A. Pomerance, W. Losert, and S. K. Gupta, "Developing a stochastic dynamic programming framework for optical tweezers based automated particle transport operations", *IEEE Trans. Automat Sci Eng*, 7, pp.218-227, 2010.

[9] K. Ramser, and D. Hanstorp, "Review article: Optical manipulation for single cell studies", *J. Biophotonics*, 3(4), pp.187-206, 2009.

[10] A. Ashkin, "History of optical trapping and manipulation of small-neutral particles, atoms, and molecules", *J. Quantum Elec.*, 6, pp.841-859, 2000.

[11] A. G. Banerjee, S. Chowhury, W. Losert, and S. K. Gupta, "Survey on indirect optical manipulation of cells, nucleic acids, and motor proteins", *J. Biomed. Optics*, 16(5): 051302, 2011.

[12] A. Stromberg, F. Ryttsen,, D. T. Chiu, M. Davidson, P. S. Eriksson, C. F. Wilson, O. Orwar, and R. N. Zare, "Manipulating the genetic identity and biochemical surface properties of individual cells with electric-field-induced fusion", *Proc. Natl. Acad. Sci. USA*, 97, pp. 7-11. 2000.

[13] F. Arai, K. Onda, R. Iitsuka, and H. Maruyama, "Multi-beam laser micromanipulation of microtool by integrated optical tweezers", *IEEE Int. Conf. Rob. & Auto.*, pp.12–17, 2009.

[14] A. G. Banerjee, A. Pomerance, W. Losert, and S. K. Gupta, "Developing a stochastic dynamic programming framework for optical tweezer based automated particle transport operations", *IEEE Trans. Automat Sci Eng*, 7, pp.218-227, 2010.

[15] S. C. Chapin, V. Germain, and E. R. Dufresne, "Automated trapping, assembly, and sorting with holographic optical tweezers", *Opt. Express*, 14(26), pp.13095-13100, 2006.

[16] Y. Wu, D. Sun, W. Huang, and N. Xi, "Dynamics analysis and motion planning for automated cell transportation with optical tweezers", *IEEE/ASME Trans. on Mechatronics*, 18(2), pp.706-713, 2013.

[17] C. Aguilar-lbanez, M. S. Suarez-Castanon, and L. I. Rosas-Soriano, "A simple control scheme for the manipulation of a particle by means of optical tweezers", *Int. J. of Robust and nonlinear control*, 21(3), pp. 328-337, 2010.

[18] S. Hu, and D. Sun, "Automatic transportation of biological cells with a robot-tweezer manipulation system", *Int. J. of robotics research*, 30(14), pp. 1681-1694, 2011.

[19] H. Chen, and D. Sun, "Moving Groups of Microparticles into array with a robot-tweezers manipulation system", *IEEE Trans. on Robotics*, 28(5), pp.1069-1080, 2012.

[20] X. Li, C. C. Cheah, S. Hu, and D. Sun, "Dynamic trapping and manipulation of biological cells with optical tweezers", *Automatica*, 49, pp. 1614-1625, 2013.

[21] X. Li, D. Sun, and J. Yang, "Bounded controller for multirobot navigation while maintaining network connectivity in the presence of obstacles", *Automatica*, 49(1), pp.285-292, 2013.

[22] D. Sun, C. Wang, W. Shang, and G. Feng, "A synchronization approach to trajectory tracking of multiple mobile robots while maintaining time-varying formations," *IEEE Trans. Robotics*, 25(5), pp. 1074-1086, 2009.

[23] Y. Wu, D. Sun, and W. Huang, "Mechanical force characterization in manipulating live cells with optical tweezers", *J. Biomechanics*, 44, pp.741-746, 2011.